Effect of oxygen concentration in the sputtering ambient on the microstructure, electrical and optical properties of radio-frequency magnetron-sputtered indium tin oxide films

1996 Semicond. Sci. Technol. 11 196

(http://iopscience.iop.org/0268-1242/11/2/009)

Semicond. Sci. Technol. **11** (1996) 196–202. Printed in the UK

Effect of oxygen concentration in the sputtering ambient on the microstructure, electrical and optical properties of radio-frequency magnetron-sputtered indium tin oxide films

Wen-Fa Wu and Bi-Shiou Chiou

Department of Electronics Engineering and Institute of Electronics, National Chiao Tung University, Hsinchu, Taiwan

Received 14 July 1995, accepted for publication 20 October 1995

Abstract. Indium tin oxide (ITO) films have been prepared by radio-frequency (rf) magnetron sputtering. The effect of oxygen concentration in the sputtering ambient on the structure and properties of ITO films are investigated. The films have a preferred orientation in the (440) plane. The presence of oxygen during sputtering enhances the crystallization of the film. Film grain size increases as more oxygen is added. According to the XPS measurements, the addition of oxygen reduces the oxygen-deficient region of the film. Hence the optical transmittance of the film is improved while film conductivity decreases.

1. Introduction

Indium tin oxide (ITO) thin films have been used as transparent conductive electrodes for many kinds of optoelectronic devices because of their high transmittance in the visible range, high infrared reflection and high electrical conductivity. Although high-quality ITO films can be prepared by a variety of methods such as sputtering, electron-beam evaporation, spray pyrolysis and screen printing, the blackening of ITO films has frequently been observed during deposition of ITO films [1–4] and/or subsequent sputtering of dielectric films on ITO-coated substrates [5–7]. This made the transparent conductive ITO films unstable during operation.

ITO is essentially an In_2O_3-based material that has been doped with Sn to improve electrical conductivity. Kobayashi *et al*, in their work on ITO/silicon oxide/Si junction solar cells, attributed the darkening of ITO to the presence of metal indium [1]. Wu and Chiou [2] and Matsuoka *et al* [5] argued that the reduction of SnO_2 in ITO films resulted in the blackening of ITO. Fan and Goodenough associated the darkening with the formation of a second phase in the bulk of the films [3]. While the mechanism for the blackening of ITO films is still not clear, the stoichiometry of the oxide film seems to be an important factor in both optical transparency and electrical conductivity. Attempts have been made to explore the correlation between the optoelectrical behaviour and the oxygen concentration of the film [8–12]. Honda *et al* argued that the oxygen content in the surface region changed considerably with the change of substrate temperature [13]. A low fabrication temperature resulted in oxygen deficiency at the film surface due to the escape of oxygen. They found a correlation between the oxygen concentration–depth profile of ITO films and the film properties. However, the detailed mechanism has not yet been revealed.

This paper reports findings from ITO films deposited by radio-frequency (rf) magnetron sputtering. The effect of oxygen concentration in the sputtering ambient on the structural and optoelectrical properties of the ITO films is investigated and discussed.

2. Experimental details

ITO films were prepared by using a commercial rf magnetron sputtering system (Ion Tech, UK). The sputtering target was a 1″ hot-pressed oxide ceramic (90 wt% In_2O_3 and 10 wt% SnO_2, 99.99% purity) supplied by Cerac, Inc., USA. The substrates employed were Corning 7059 glass, degreased ultrasonically in a dilute detergent solution, rinsed ultrasonically in deionized water and blown dry in N_2 gas before they were introduced

0268-1242/96/020196+07$19.50

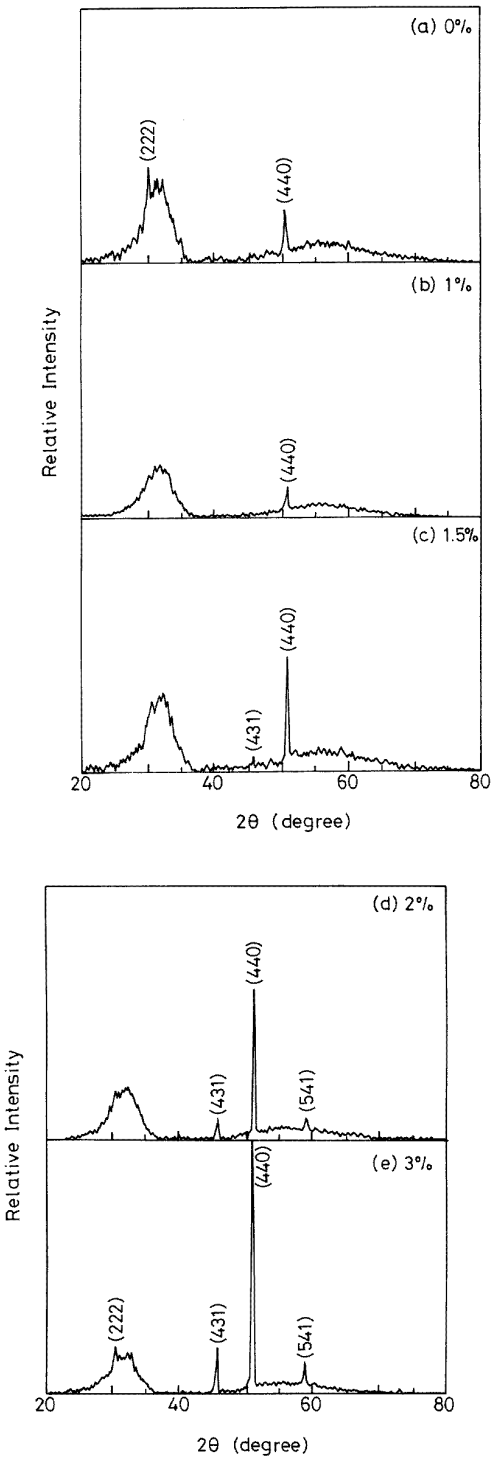

Figure 1. X-ray diffraction patterns for the as-deposited ITO films prepared under various oxygen percentages. Film thickness ∼ 8000 Å, sputtering power 60 W.

into the chamber. The substrate was fixed directly above the target with a target-to-substrate distance of 6 cm and a mechanical shutter was attached to the target. During sputtering, the substrate temperature was between 70 and 80 °C.

The vacuum chamber was a stainless steel bell jar pumped by a conventional oil diffusion pump (Diffstak 250, Edwards, UK). High-purity Ar (99.999%) and O_2 (99.5%) were introduced through a mass flow controller after the vacuum chamber was evacuated to about 2×10^{-6} Torr. The gas pressure was monitored with a precision ionization gauge and was kept at 7.5×10^{-3} Torr during deposition. The rf power (13.56 MHz) was introduced through an rf power supply (RF Plasma Products, Inc., USA) with an automatic matching network which could be tuned for minimum reflected power. Before deposition, the target was presputtered to remove any contaminants and eliminate any differential sputtering effects. The presputtering time was 20 min for pure Ar and was increased to 30 min as O_2 was added to the sputtering ambient.

The film thickness was measured with a stylus surface profiler. The sheet resistance of the samples was measured with a four-point probe and the resistivity of the film was calculated. Carrier concentration and Hall mobility were obtained from Hall effect measurement by the van der Pauw technique. An x-ray diffractometer was used to identify the crystalline phase of the films. Chemical binding energy analysis was performed using an x-ray photoemission spectroscope (XPS, Perkin PHI-590AM SAM/1905 ESCA, Massachusetts, USA) with an Mg K_α x-ray source. The microstructure of the films was analysed using a scanning electron microscope (SEM, Hitachi S-4000, Japan). The optical transmittance of the films was measured with an ultraviolet–visible–near infrared spectrophotometer (Hitachi U-3410, Japan).

3. Results and discussion

The x-ray diffraction patterns for as-deposited films prepared at various oxygen percentages are shown in figure 1, where the peak (440) is the most prominent for all films, suggesting that the films have a strong (440) texture. The relative (440) crystal plane intensity increases with increasing oxygen percentage from 0% to 3%. It is evident that the presence of oxygen in the sputtering atmosphere enhances the crystallinity of the film since the apparent crystalline characteristics are observed after oxygen is added. This enhanced crystallization with added oxygen has been observed previously [14–17]. However, the preferred orientation, reported by Kumar and Mansingh, at an oxygen concentration of more than 10% was the (222) crystal plane.

X-ray photoemission spectroscopy (XPS) measurements were carried out to find chemical bonding states of ITO films. The position of the carbon 1s peak is taken as a standard (binding energy = 284.6 eV) to compensate for any charge-induced shifts. The In 3d, Sn 3d and O 1s XPS spectra of the as-deposited ITO films prepared at various oxygen percentages are shown in figures 2, 3 and 4, respectively. As shown in figure 2, the binding energies of the In $3d_{5/2}$ and In $3d_{3/2}$ levels are 444.4 and 452.0 eV respectively. No appreciable difference is observed between ITO films prepared under different oxygen percentages. The conductivity of ITO is n-type as a result of oxygen vacancies and the presence of tin dopant which

Table 1. O 1s peaks for ITO films prepared under various oxygen percentages.

Oxygen percentage (%)	Positions (eV)		Relative strengths (%)		Peak ratios
	O_I	O_{II}	O_I	O_{II}	O_I/O_{II}
0	531.4	529.8	44.09	55.91	∼0.8
2	531.5	529.8	35.95	64.05	∼0.6
3	531.4	529.9	38.38	61.62	∼0.6

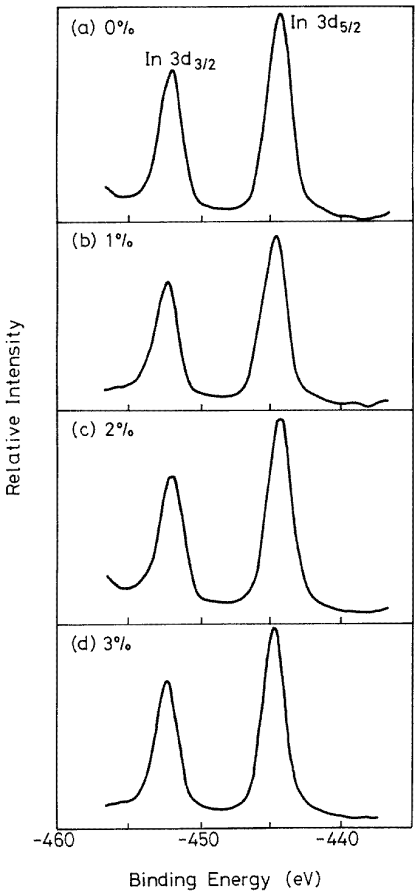

Figure 2. In 3d XPS spectra of the as-deposited ITO films prepared under various oxygen percentages.

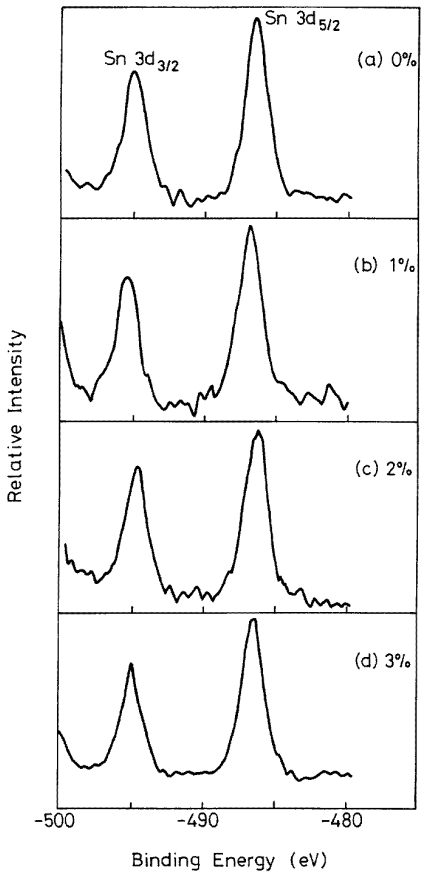

Figure 3. Sn 3d XPS spectra of the as-deposited ITO films prepared under various oxygen percentages.

has a higher valence than indium. The generation of n-type charge carriers, i.e. electrons, can be described as follows:

$$O_O \rightarrow V_O^{\cdot\cdot} + 2e' + \tfrac{1}{2}O_{2(g)} \qquad (1)$$

$$2SnO_{2(s)} \xrightarrow{In_2O_3} 2Sn_{In}^{\cdot} + 3O_O + 2e' + \tfrac{1}{2}O_{2(g)}. \qquad (2)$$

Since the extra electronic charge in the ITO films is trapped only at V_o (oxygen vacancies) and Sn centres, the In $3d_{3/2}$ and In $3d_{5/2}$ peaks should be insensitive to the loss of oxygen and to the Sn concentration [3]. It is reported in the literature [18] that the In 3d peak for metallic indium is observed at energies 0.4–1.4 eV lower than that for In_2O_3. There is some asymmetry of the peaks, indicating that a multiple component may be present. Nelson and Aharoni [19] reported that the XPS In $3d_{5/2}$ peak can be resolved into two peaks which are separated by approximately 1.0 eV. The positions of the two resolved peaks in the In $3d_{5/2}$ spectra are located at 443.7 and 444.6 eV. They suggested that the lower-energy peak, located at 443.7 eV, corresponds to the In^0 bonding state, specifically In–In bonds, and the higher-energy peak, located at 444.6 eV, corresponds to the In^{3+} bonding state, specifically In_2O_3.

As shown in figure 3, almost the same Sn $3d_{3/2}$ and Sn $3d_{5/2}$ spectra are observed for the as-deposited ITO films prepared under various oxygen percentages. Two peaks due to Sn $3d_{3/2}$ and Sn $3d_{5/2}$ are located at 495.0 ± 0.2 and 486.4 ± 0.2 eV respectively. Fan and Goodenough [3] reported that the Sn 3d peak for Sn^{2+} in SnO is observed at an energy 0.5 eV higher than that for Sn^{4+} in SnO_2, whereas the Sn 3d peak for metallic tin is observed at an energy 1.8 eV lower than the Sn^{4+} 3d peak. Thermodynamically

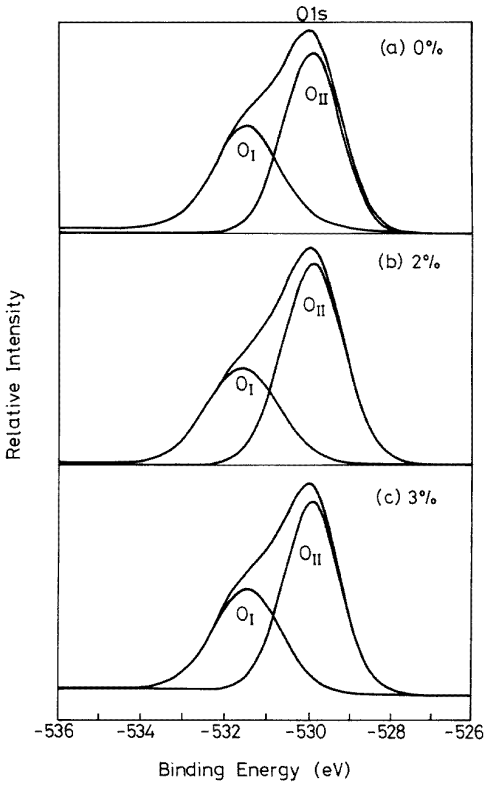

Figure 4. O 1s XPS spectra of the as-deposited ITO films prepared under various oxygen percentages.

SnO_2 is more stable than SnO, and thus Sn^{4+} is thought to be the predominant state in the ITO films. Fan and Goodenough suggested that the darkening of the rf sputtered ITO films was caused by the formation of the Sn_3O_4 phase. However, no evidence for an Sn_3O_4-like phase exists in the present work.

Figure 4 shows the XPS O 1s spectra of the as-deposited ITO films prepared under various oxygen percentages. A shoulder appears on the higher-energy side of the main peak for the O 1s spectra in all samples. The deconvoluted O 1s spectra allow one to distinguish between a peak located at around 531.5 eV (referred to as O_I) and a peak around 529.9 eV (referred to as O_{II}). The corresponding deconvoluted peaks are indicated by full curves as shown in figure 4. The resolution procedure for the oxygen 1s peak uses two Gaussian functions with variable positions, widths and intensities. Table 1 summarizes the corresponding results. The relative strengths are obtained by comparing the integrated areas of the O_I and O_{II} peaks. As can be seen in table 1, the peak ratio of O_I and O_{II} states becomes smaller as the oxygen is added during sputtering.

In_2O_3 crystallizes with a bixbyite, C-type cubic, rare earth sesquioxide crystal structure with space group $T_h^7 Ia3$ [3, 20]. Each indium atom is surrounded by six oxygen atoms at the corners of a distorted cube, with two vacancies at the two unoccupied corners. Previous works suggested that the lower-energy peak located at $\sim$ 530.0 eV corresponds to O^{2-} ions which have neighbouring In atoms with their full complement of six nearest-neighbour O^{2-} ions, and the higher-energy peak located at $\sim$ 532 eV

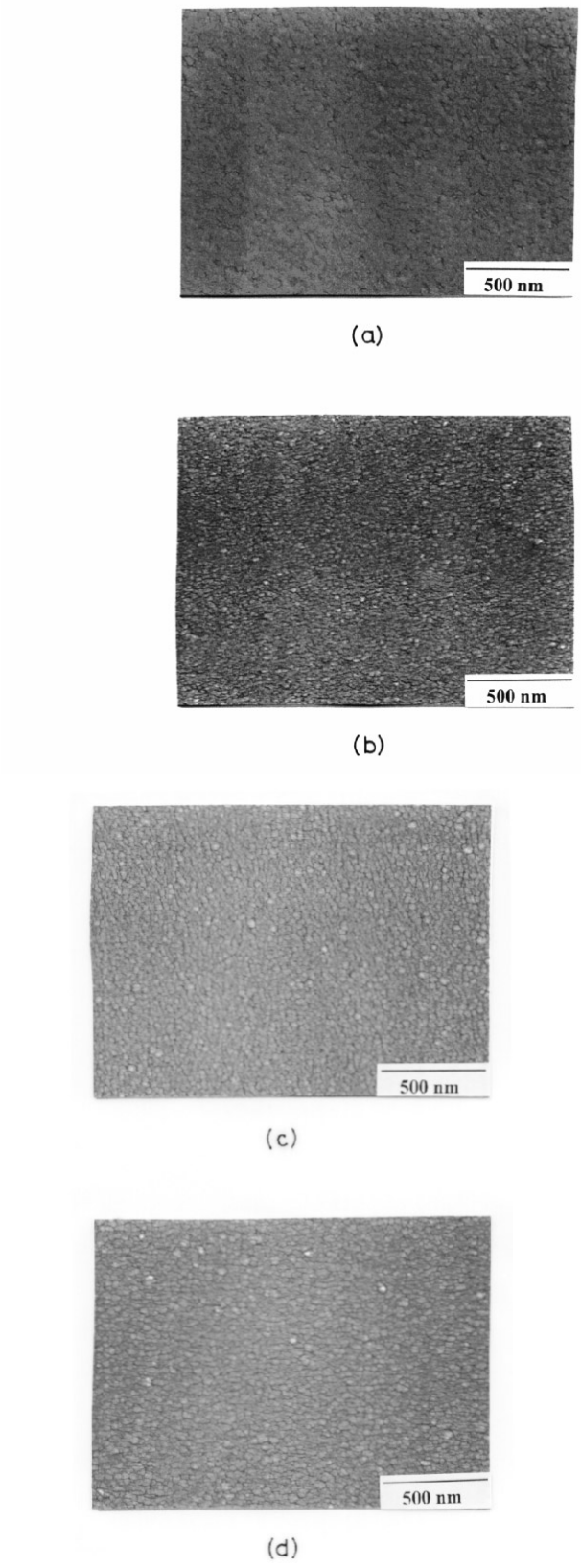

Figure 5. SEM micrographs of ITO films prepared under various oxygen percentages. Film thickness $\sim$ 2000 Å, sputtering power 100 W.

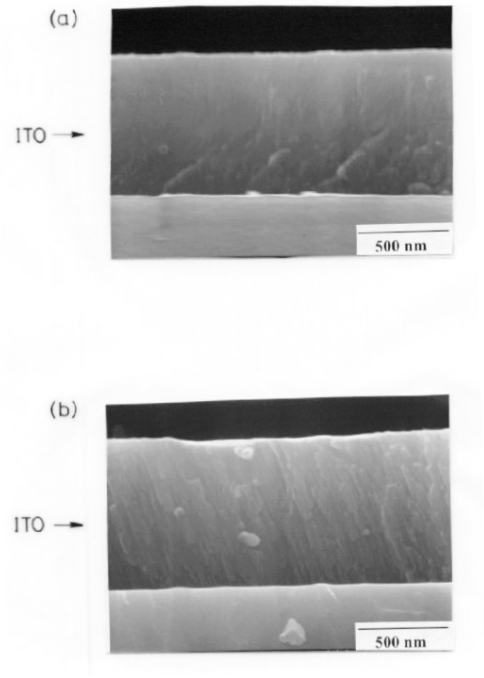

Figure 6. Cross-sectional SEM micrographs of ITO films prepared under various oxygen percentages: (*a*) 0% and (*b*) 2%. Film thickness ∼ 8000 Å.

corresponds to O^{2-} ions in an oxygen-deficient region [3, 4]. Nelson and Aharoni proposed another possible explanation for the higher-energy peak and suggested that the higher-energy peak located at ∼ 532 eV may represent the existence of O–Sn bonds based on other group IV oxides [19]. In the study, the main peak O_{II} can be assigned to an O–In bonding state in which In ions are fully bonded with neighbouring O^{2-} ions. As for the subpeak O_I, there are two possible explanations: (i) a peak associated with an O–In bonding state in the oxygen-deficient region or (ii) tht with an O–Sn bonding state. Since the O_I peak decreases as oxygen is added to the sputtering ambient, the former explanation is more reasonable in this case.

Figure 5 shows SEM micrographs of ITO films prepared under various oxygen percentages. It is seen in figure 5 that grain size increases as oxygen concentration in the sputtering ambient increases from 0 to 2%, while no apparent difference in grain size is observed between 2 and 3%. The addition of oxygen enhances crystallization of the films, as confirmed by the results of x-ray diffraction experiments. Figure 6 illustrates the cross-sectional SEM micrographs of ITO films ∼ 8000 Å thick prepared at 0 and 2% oxygen. As shown in figure 6, an apparent columnar structure is found. For the ITO film prepared under 0% oxygen, a grainy structure appears on the lower part of the film and the columnar structure develops at about half of the film thickness, while ITO films prepared at 2% show a highly columnar structure in all regions.

Figure 7 gives the resistivity, charge carrier concentration and Hall mobility of ITO films as function of oxygen percentage. The resistivity increases as oxygen pressure increases. This is attributed to the combined effect of changes

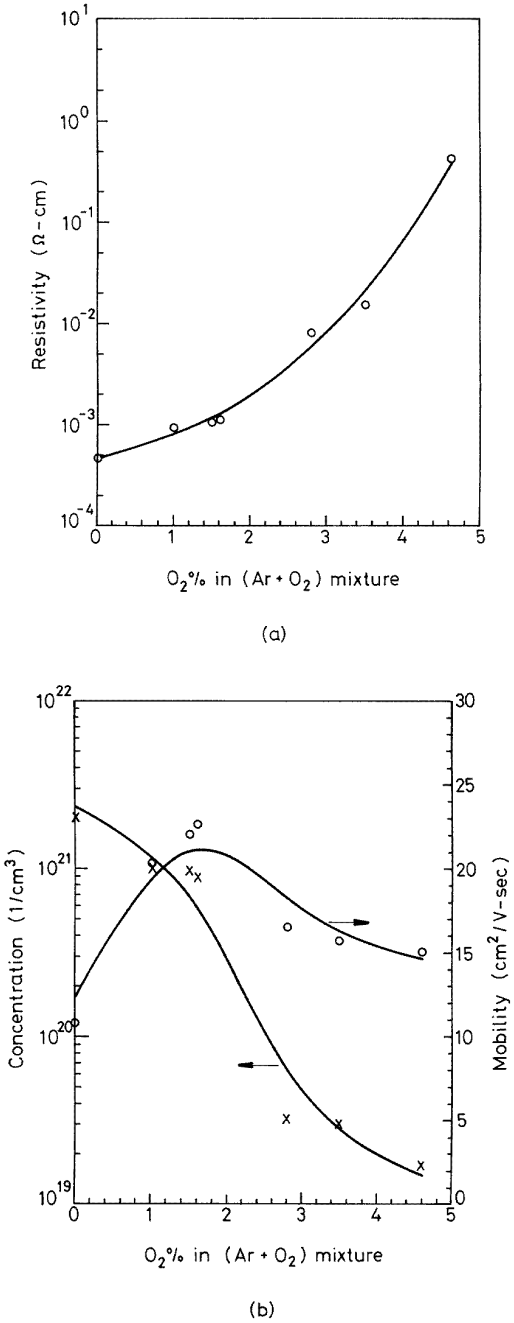

Figure 7. (*a*) Resistivity and (*b*) charge carrier concentration and Hall mobility of ITO films as a function of oxygen percentage.

in carrier concentration and Hall mobility. The carrier concentration of the ITO films decreases and Hall mobility increases initially and then decreases as the oxygen percentage increases from 0 to 4.6% as shown in figure 7(*b*). The incorporation of oxygen leads to a decrease in oxygen vacancies in the films and hence to a fall in the carrier concentration. The electron mobility is affected by the structure of the film. Surface morphology and crystallinity are important factors of crystal structure. The increase in mobility with increasing added oxygen may result from grain size effects [15]. As observed in figure 5, the grain size

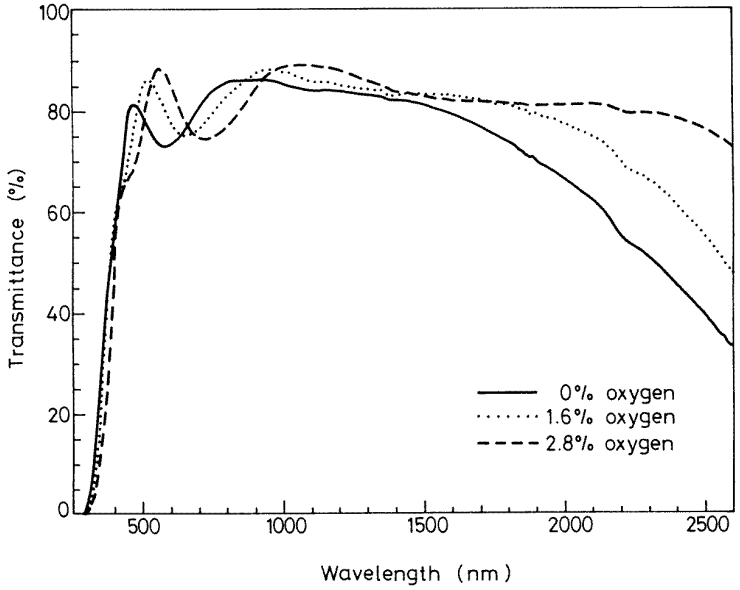

Figure 8. Transmittance of ITO films prepared under various oxygen percentages.

of the ITO film increases with increase in oxygen percentage, hence scattering from grain boundaries becomes less important for films prepared under a higher oxygen concentration. Consequently, the mobility increases as the oxygen percentage increases. However, with further increase in oxygen pressure, added oxygen can damage the film by introducing defects because an Sn^{+4} ion pair may attract an additional oxygen atom, producing a neutral cluster $(SnO_2)_2$ in which the additional oxygen atoms play the role of electron traps and so reduce the carrier mobility as observed in figure 7(*b*) [21].

Figure 8 shows the transmittance of the as-deposited film prepared under various oxygen percentages. The visible transmittance of the film is enhanced as more oxygen is added. In previous work it was argued that the oxygen deficiency in the ITO film would contribute to blackening of the ITO film [4, 5], hence the blackening of the ITO film would be improved as oxygen gas is added and the transmittance of the ITO films increases with the addition of oxygen, as observed.

Although introducing oxygen gas during deposition would enhance the transmittance of the film, too high an oxygen pressure has presumably too few oxygen vacancies to act as charge carriers as described in equation (1). The critical role of the partial oxygen pressure can be naturally explained as the conflicting requirements of introducing enough oxygen vacancies without creating too large an absorption.

In addition to increasing the visible transmission of the films, increasing the oxygen partial pressure during deposition results in a shift of the intrinsic absorption edge to a longer wavelength as seen in figure 8. This shift is due to the decrease in carrier concentration, which lowers the Fermi level and reduces the magnitude of the Burstein effect [22, 23].

4. Conclusion

The structural orientation of rf magnetron-sputtered ITO films depends on the oxygen percentage in the sputtering ambient. The films have a preferred orientation in the (440) plane. The presence of oxygen in the sputtering atmosphere enhances the crystallinity of the film and increases the film grain size. XPS results indicate a reduction in the oxygen-deficient region of the ITO films as oxygen is added during sputtering.

The charge carrier mobility of the film increases initially and then decreases as oxygen pressure increases. The initial increase in mobility is attributed to the reduced grain boundary scattering resulting from the large grain size, while the decrease in mobility is caused by the trapping effect of the neutral cluster $(SnO_2)_2$ when the oxygen percentage is further increased.

Blackening of ITO is reduced with the addition of oxygen, but too much oxygen raises film resistivity. The oxygen partial pressure plays a critical role. It has to fulfil the conflicting requirements of introducing enough oxygen vacancies for electrical conduction without creating too large an optical absorption.

Acknowledgments

This work is supported by the Chung-Shan Institute of Science and Technology (contract no CS 83-0210-D-009-001) and partly supported by the National Science Council of Taiwan, Republic of China (contract no NSC 82-0417-E009-395).

References

[1] Kobayashi H, Ishida T, Nakamura K, Nakato Y and Tsubomura H 1992 *J. Appl. Phys.* **72** 5288

[2] Wu W F and Chiou B S 1994 *Thin Solid Films* **247** 201
[3] Fan J C C and Goodenough J B 1977 *J. Appl. Phys.* **48** 3524
[4] Wu W F, Chiou B S and Hsieh S T 1994 *Semicond. Sci. Technol.* **9** 1242
[5] Matsuoka T, Kuwata J, Fujita Y and Abe A 1988 *Japan. J. Appl. Phys.* **27** L1199
[6] Chubachi Y and Aoyama K 1991 *Japan. J. Appl. Phys.* **30** 1442
[7] Panicker M P R and Essinger W F 1981 *J. Electrochem. Soc.* **128** 1943
[8] Ichihara K and Okubo M 1994 *Japan. J. Appl. Phys.* **33** 4478
[9] Ichihara K, Inoue N, Okubo M and Yasuda N 1994 *Thin Solid Films* **245** 152
[10] Davis L 1993 *Thin Solid Films* **236** 1
[11] de Andrade A C and Moehlecke S 1994 *Appl. Phys.* A **58** 503
[12] Honda S, Tsujimoto A, Watamori M and Oura K 1994 *Japan. J. Appl. Phys.* **33** L1257
[13] Honda S, Tsujimoto A, Watamori M and Oura K 1995 *J. Vac. Sci. Technol.* A **13** 1100
[14] Vasant Kumar C V R and Mansingh A 1989 *J. Appl. Phys.* **65** 1270
[15] Buchanan M, Webb J B and Williams D F 1980 *Appl. Phys. Lett.* **37** 213
[16] Higuchi M, Sawada M and Kuronuma Y 1993 *J. Electrochem. Soc.* **140** 1773
[17] Dutta J and Ray S 1988 *Thin Solid Films* **162** 119
[18] Ishida T, Kobayashi H and Nakato Y 1993 *J. Appl. Phys.* **73** 4344
[19] Nelson A J and Aharoni H 1987 *J. Vac. Sci. Technol.* A **5** 231
[20] Elfallal I, Pilkington R D and Hill A E 1993 *Thin Solid Films* **223** 303
[21] Martínez M A, Herrero J and Gutiérrez M T 1992 *Solar Energy Mater*. **26** 309
[22] Wu W F and Chiou B S 1993 *Appl. Surf. Sci.* **68** 497
[23] Burstein E 1954 *Phys. Rev.* **93** 632